Supporting Information

Tunable hydrogen production of transition metal anchored $CuInP_2S_6$ monolayer with ferroelectric switch

Shiqi Huang[1], Tingting Bo[2], Nan Mu[2], Shiyu Liu[1], Wei Zhou[2], Dejun Li[1*], Yanyu Liu[1*]*

1. College of Physics and Materials Science, Tianjin Normal University, Tianjin, 300387, P. R. China.

2. Department of Applied Physics, Tianjin Key Laboratory of Low Dimensional Materials Physics and Preparing Technology, School of Science, Tianjin University, Tianjin 300072, P. R. China.

***E-mail: weizhou@tju.edu.cn; dejunli@tjnu.edu.cn; yyliu@tjnu.edu.cn**

1. Calculation method for solar-to-hydrogen efficiency

The calculation of solar-to-hydrogen (STH) efficiency (η_{STH}) is as follows [1]:

$$\eta_{STH} = \eta_{abs} \times \eta_{cu}$$

where η_{abs} is the light absorption efficiency, η_{cu} is the carrier utilization rate. They are defined as:

$$\eta_{abs} = \frac{\int_{E_g}^{\infty} P(h\omega)d(h\omega)}{\int_{0}^{\infty} P(h\omega)d(h\omega)}$$

$$\eta_{cu} = \frac{\Delta G_{H_2O} \int_{E}^{\infty} \frac{P(h\omega)}{h\omega} d(h\omega)}{\int_{E_g}^{\infty} P(h\omega)d(h\omega)}$$

$P(h\omega)$ is the solar flux of the reference atmospheric mass 1.5 global spectrum (AM1.5G) at photon energy $h\omega$, and E_g is the direct band gap value of the catalyst. It should be noted that the band gap value here needs to be obtained under the HSE06 hybrid functional. The denominator represents the total power density of the reference sunlight spectrum, and the numerator represents the light power density absorbed by the catalyst.

In the definition of η_{cu}, ΔG_{H_2O} is the free energy of water decomposition, its size is 1.23 eV, and the molecule represents the effective photocurrent density. E represents the photon energy that can actually be utilized in the water decomposition process, and its value can be obtained by the following formula when evaluating different material systems:

$$E = \begin{cases} E_g, (\chi(H_2) \geq 0.2, \chi(O_2) \geq 0.6)) \\ E_g + 0.2 - \chi(H_2), (\chi(H_2) \\ E_g + 0.6 - \chi(O_2), (\chi(H_2) \geq 0.2, \chi(O_2) < 0.6)) \\ E_g + 0.8 - \chi(H_2) - \chi(O_2), (\chi(H_2) < 0.2, \chi(O_2) < 0.6)) \end{cases}$$

where $\chi(H_2)$ represents the over-potential of hydrogen evolution reaction, that is, the energy difference between the conduction band bottom of the catalyst and the H^+/H_2 reduction potential (-4.44 eV); $\chi(O_2)$ represents the overpotential of the oxygen evolution reaction, that is, the energy difference between the valence band top of the catalyst and the H_2O/O_2 oxidation potential (-5.67 eV).

However, the intrinsic electric field inherent in ferroelectric materials plays a key role in the separation of electron-hole pairs, and this effect can improve the separation efficiency of photogenerated carriers. Therefore, when evaluating the η_{STH} of ferroelectric materials for photocatalytic water decomposition, the energy contribution of the intrinsic electric site must be included in the total energy calculation, where $\eta_{STH}^{'}$ is:

$$\eta_{STH}^{'} = \eta_{STH} \times \frac{\int_0^{\infty} P(h\omega)d(h\omega)}{\int_0^{\infty} P(h\omega)d(h\omega) + \Delta V \int_{E_g}^{\infty} \frac{P(h\omega)}{h\omega} d(h\omega)}$$

where ΔV is the electrostatic potential difference between the two sides of the ferroelectric material.

2. Calculation method for the polarization intensity

The polarization intensity of $CuInP_2S_6$ is calculated by using the modern polarization theory based on the Berry phase method[2~4]. Due to the Born-Karman periodic boundary condition, the spontaneous polarization is affected by the polarization quantum ($P_q = eR/\Omega$), where e is the charge of the electron, R is the lattice constant in the polarization direction, and Ω is the volume of the unit cell. Then the calculation

formula of spontaneous polarization is as follows:

$P_s = P_{fin} + nP_q + P_{int}$

where, n is an arbitrary integer, P_{fin} is the polarization of the FE structure in the final state, and P_{int} is the polarization of the PE structure in the initial state.

The core of the Berry phase method is to determine the polarization intensity of the material by calculating the Berry phase of the electron wave function. The relationship between Berry phase and polarization can be described by the following formula:

$$P = \frac{e}{\Omega}\sum_n f_n \int_{BZ} dk A_n(k)$$

where, P is the polarization intensity, e is the electron charge, Ω is the unit cell volume, f_n is the occupation number of the nth energy band, and $A_n(k)$ is defined as:

$A_n(k) = i\langle u_{n,k} \left| \nabla_k \right| u_{n,k} \rangle$

$u_{n,k}$ is the periodic part of the Bloch function.

Table S1. Bond length of TM-S under AIMD simulation (Å).

	d_{TM-S4}	d_{TM-S5}	d_{TM-S6}
Anchored	2.08	2.09	2.30
100 K~300 K	2.18	2.35	2.28
300 K	2.08	2.29	2.27

Table S2. Calculation parameters for the solar-to-hydrogen efficiency.

Materials	$\chi(H_2)$	$\chi(O_2)$	ΔV
$CuInP_2S_6$	0.457 eV	1.106 eV	0.41 V
$Cr@CuInP_2S_6$	0.166 eV	0.334 eV	0.45 V
$Fe@CuInP_2S_6$	0.343 eV	0.309 eV	0.52 V

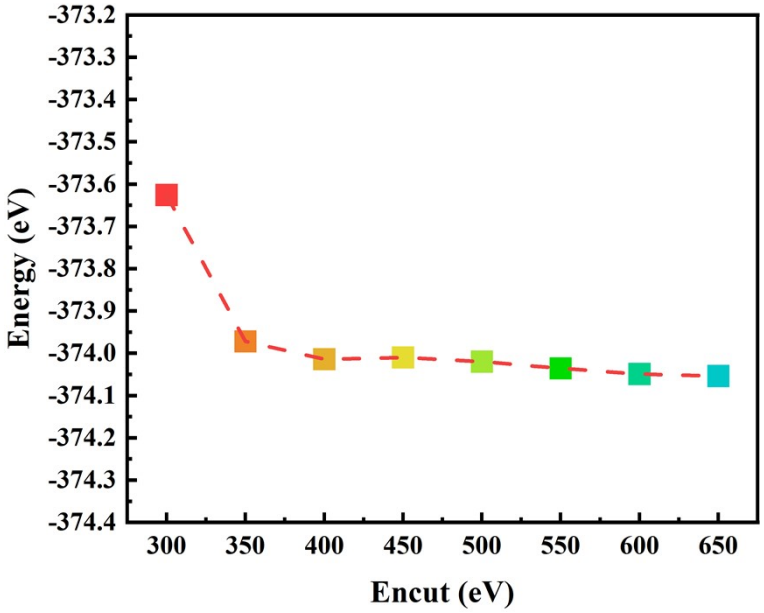

Figure S1. The cut-off energy test of $CuInP_2S_6$ monolayer.

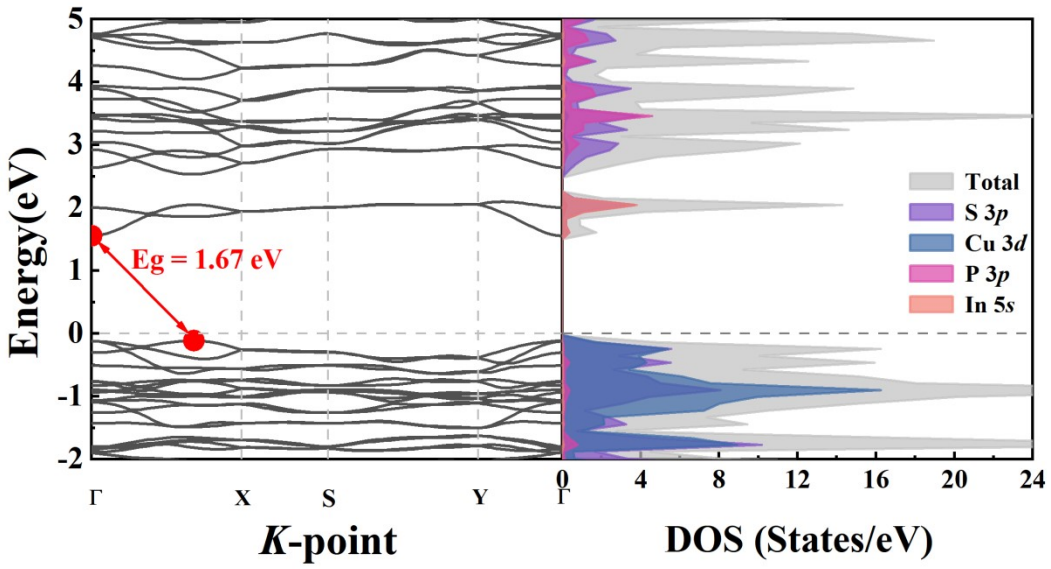

Figure S2. The band structure and DOS of the $CuInP_2S_6$ monolayer from PBE method.

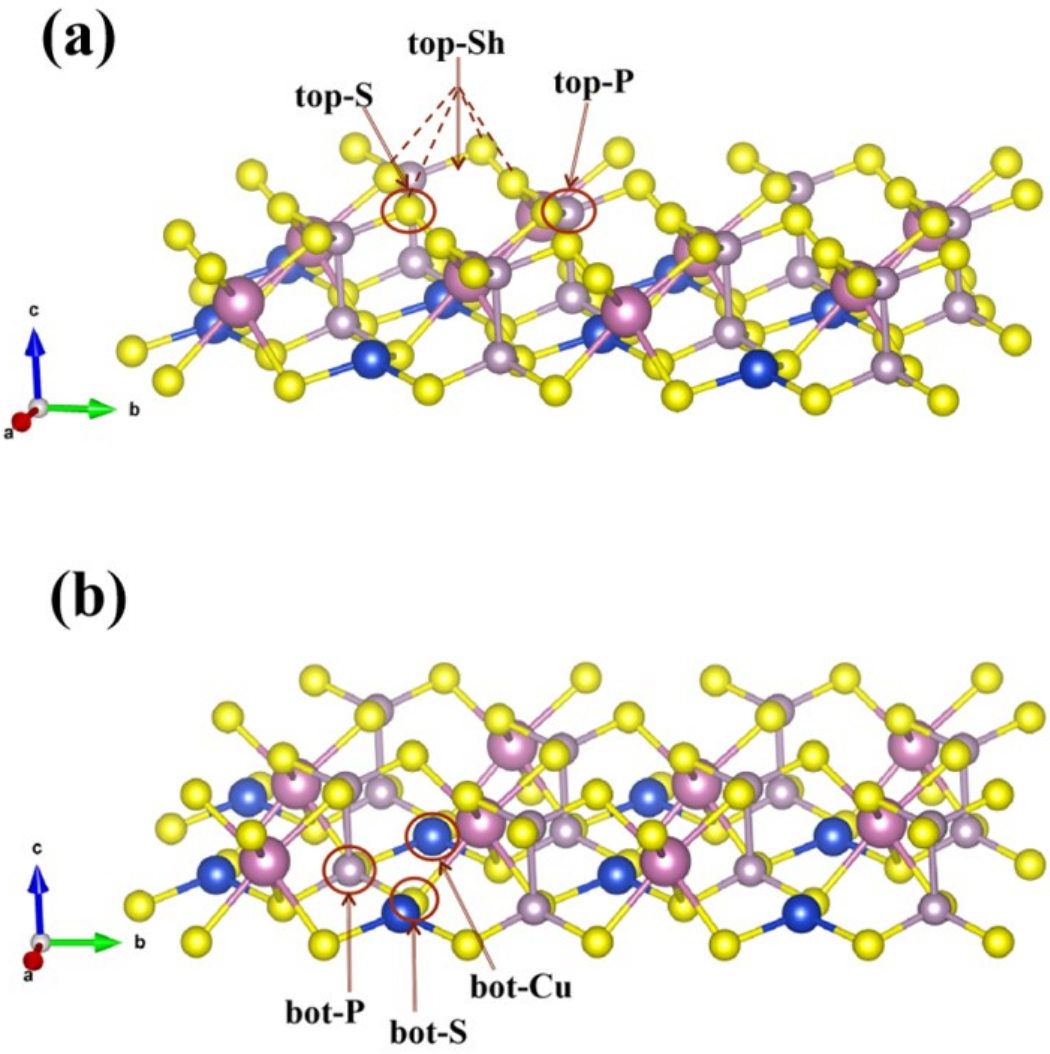

Figure S3. Six reaction sites on the $CuInP_2S_6$ monolayer. (a) Sites on the top surface and (b) sites on the bottom surface.

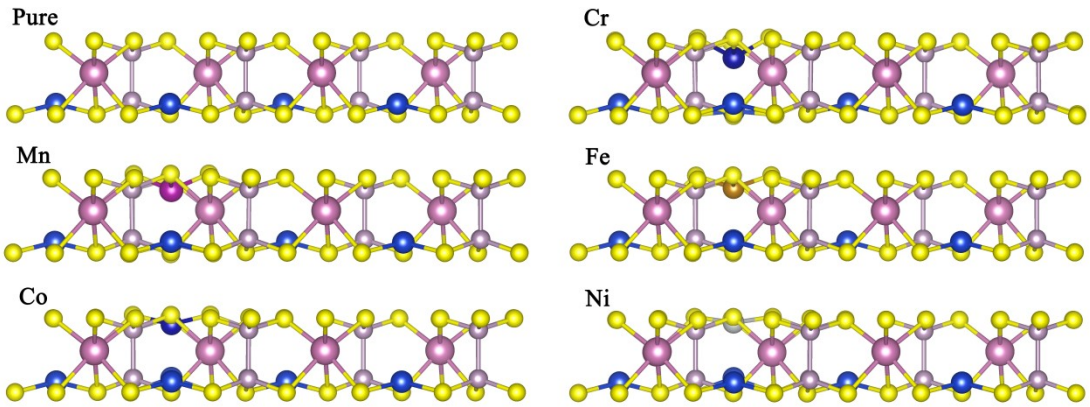

Figure S4. Structures of TM (TM = Cr, Mn, Fe, Co, Ni) anchored on the top surface of $CuInP_2S_6$ monolayer.

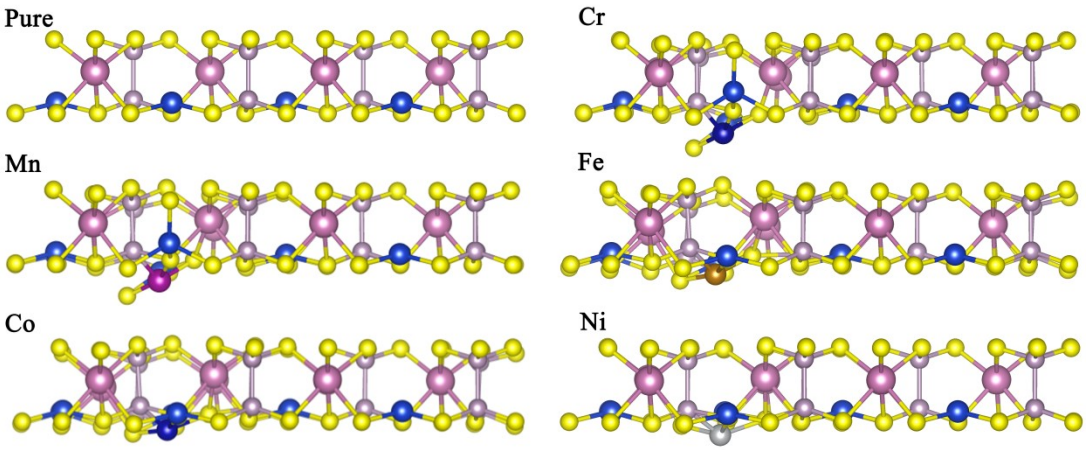

Figure S5. Structures of TM (TM = Cr, Mn, Fe, Co, Ni) anchored on the bottom surface of $CuInP_2S_6$ monolayer.

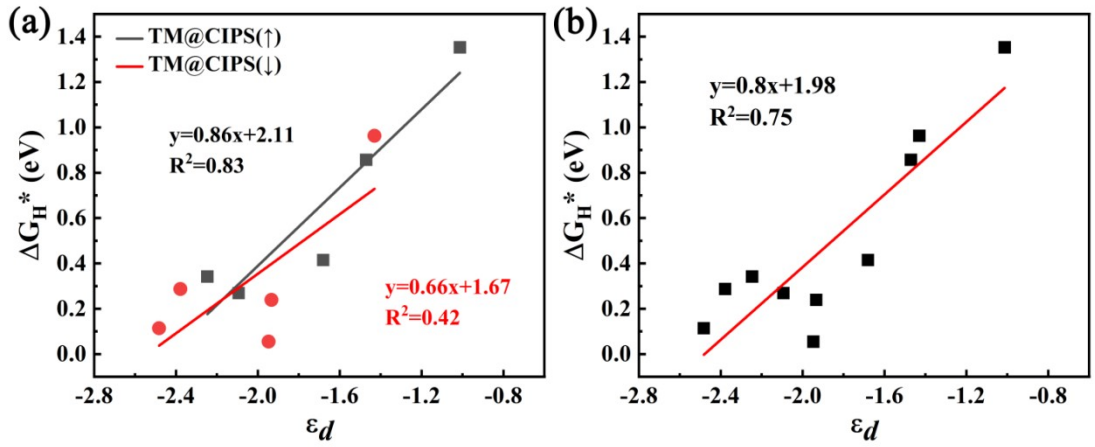

Figure S6. The hydrogen adsorption free energy of TM@$CuInP_2S_6$ system. (a) ΔG_{H^*} and ε_d are fitted separately according to polarization direction. The black and red lines represent the upward polarization and downward polarization anchored systems, respectively. (b) ΔG_{H^*} and ε_d are fitted regardless of polarization direction.

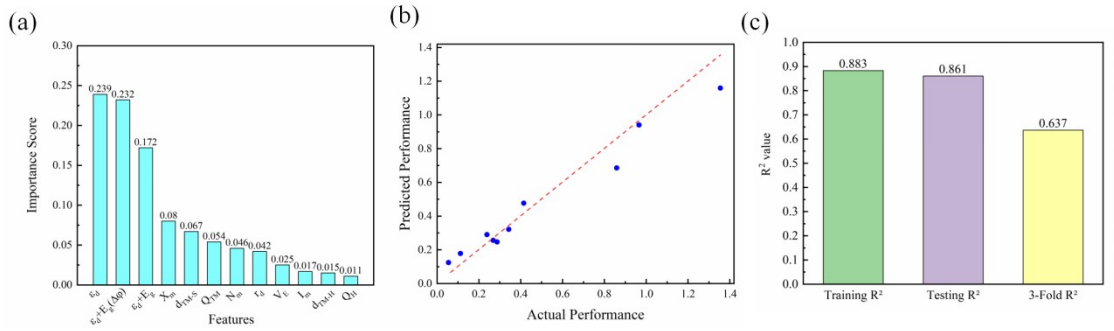

Figure S7. (a) Verification of the feature importance of the random forest algorithm by the permutation test method. (b) Linear fitting between model prediction and actual performance (R^2 = 0.95). (c) 3-cross validation for the result of machine learning.

The optimized POSCAR and the necessary INCAR files:

The optimized POSCAR of pure-phase $CuInP_2S_6$.

CIPS\(2)\(0\0\1)

1.00000000000000

6.0876172674654532 0.0000000000000000 0.0000000000000000

0.0000000000000000 10.5588870036033722 0.0000000000000000

0.0000000000000000 0.0000000000000000 19.4197006226000006

Cu In P S

2 2 4 12

Direct

0.9202189153586176 0.5851697508260045 0.4367624297037764

0.4202188763586179 0.0851697398260001 0.4367624297037764

0.4179517461902691 0.7513697476329639 0.5109311847289177

0.9179517461902691 0.2513697476329639 0.5109311847289177

0.9191747938473824 0.9184127964594353 0.4439245809480283

0.4191747548473899 0.4184128414594355 0.4439245809480283

0.9180980055899397 0.9181249238178708 0.5595154543246394

0.4180979655899435 0.4181248788178706 0.5595154543246394

0.5979282631907381 0.9058750629670413 0.4119675351767782

0.0979282231907419 0.4058750179670412 0.4119675351767782

0.0618967417288943 0.0853211983205995 0.4124355716406356

0.5618967517288951 0.5853211693206006 0.4124355716406356

0.0993223364526017 0.7640126115973374 0.4122109117022958

0.5993223264526009 0.2640126115973374 0.4122109117022958

0.2389994220027205 0.9271498621447307 0.5865573727478193

0.7389994800027253 0.4271499071447309 0.5865573727478193

0.7427962609975154 0.0736184080828082 0.5861383974228787

0.2427962219975157 0.5736184080828082 0.5861383974228787

0.2717336836413082 0.2528756421512171 0.5859965616042331

0.7717336636413066 0.7528756421512171 0.5859965616042331

The optimized POSCAR of TM@$CuInP_2S_6$(↑), taking Ni@$CuInP_2S_6$(↑).

2\2\1\CIPS

1.00000000000000

12.1752004622999994 0.0000000000000000 0.0000000000000000

0.0000000000000000 21.1177997588999986 0.0000000000000000

0.0000000000000000 0.0000000000000000 19.4197006226000006

Cu In P S Ni

8 8 16 48 1

Direct

0.4580517997111886 0.2924744521994883 0.4470244821320097

0.2078028034213476 0.0423389629791118 0.4368805320799433

0.9578026832382268 0.2927438443765178 0.4369259931411840

0.7081592638271352 0.0418767990652515 0.4363161611165420

0.4586313033700069 0.7922801071989325 0.4363962261525117

0.2082073307751745 0.5427533416886476 0.4370607192912278

0.9583659615970478 0.7923884265930310 0.4365879820396430

0.7096162916996650 0.5426312657692339 0.4366863206175708

0.2062426846798562 0.3764449699151142 0.5088656974156492

0.4583905540653980 0.1241438995127841 0.5088406575523485

0.7103818078383577 0.3764286049655917 0.5084781071573427

0.9585119101788684 0.1253959304966434 0.5099938108565275

0.2080931566588918 0.8756532409164584 0.5107490784436501

0.4581442615443553 0.6257970401701179 0.5106617409814471

0.7084219713913641 0.8751557324442439 0.5104686433488816

0.9588266907212025 0.6259570745373910 0.5102666543835677

0.4591796472913197 0.4585721810654113 0.4450576166678263

0.2088298158012367 0.2097387058606295 0.4446443413625781

0.4590373341037145 0.4591199581775439 0.5608906575915648

0.2080188385316263 0.2092335920636112 0.5604495499205289

0.9586462515149488 0.4595950740533779 0.4429029323315667

0.7068899918466399 0.2089379158481414 0.4444411076725712
0.9585905344560219 0.4602469990614705 0.5585904984683522
0.7088748517984508 0.2087971258671269 0.5602513884666092
0.4580461537499023 0.9584560574194175 0.4433338102461258
0.2086354798716007 0.7091745053450111 0.4437593966085449
0.4583402608309655 0.9579566411805085 0.5589818692895453
0.2083263985005298 0.7090881225569983 0.5593813749130345
0.9581312662376066 0.9589246730699448 0.4433376162429174
0.7084389449696880 0.7088714569736465 0.4435997897281150
0.9581046155949903 0.9591381918850648 0.5589485514272807
0.7085669724756410 0.7087383652836942 0.5592233677714694
0.2987083922013550 0.4536941888341675 0.4123264069183137
0.0477446347020632 0.2034622549174558 0.4129096156373081
0.0290417553437446 0.0423111693436793 0.4112891368906940
0.2807887623492407 0.2922727594964113 0.4124702706486285
0.0476543389867747 0.3817834491944758 0.4112255469468182
0.2966045097930347 0.1319406676432391 0.4121246012050557
0.1187691998214734 0.4661861910806297 0.5845906312607343
0.3722879364846889 0.2070879422228492 0.5925722941205503
0.3710541854910868 0.0353495784170970 0.5859329455077074
0.1250241169232900 0.2879503739359818 0.5880952506967152
0.1352701758726973 0.1261881323890100 0.5856914930622547
0.3735951489263635 0.3780362719275421 0.5927032482040117
0.7978870907146839 0.4531709191992072 0.4105998562643191
0.5467881289893853 0.2037832110935801 0.4126258690983675
0.5294064796682939 0.0419689449911173 0.4113358994427915
0.7792313907324222 0.2917024045286352 0.4115606802069449
0.5467572358531014 0.3811858698483110 0.4127869662223403
0.7969443080341948 0.1315613310318693 0.4127417342825072
0.6186339242883208 0.4607167040163273 0.5884704665251950

0.8700978707842887	0.2139134826106987	0.5853368720164356
0.8704032146060761	0.0369344272814165	0.5854900974247940
0.6299358133217660	0.2917738500231395	0.5925233612239600
0.6323632146302336	0.1279256509916078	0.5878075874719985
0.8874154010587375	0.3774244847982359	0.5852148080044403
0.2970571776048281	0.9528221039091502	0.4118259614994733
0.0477836677550358	0.7029690537297094	0.4119252256982684
0.0297150085125561	0.5427724649172712	0.4106673227581012
0.2795584194828063	0.7925845123194816	0.4120382919587764
0.0481953985414061	0.8816474213568730	0.4119537364360847
0.2982339888645790	0.6318940053306873	0.4120010275712537
0.1188255639853946	0.9641400756098616	0.5856035946939567
0.3687249994487609	0.7135094024310776	0.5864429776150969
0.3716005333497889	0.5371803424402608	0.5866002114063074
0.1207179279133620	0.7868730119173848	0.5860335079971959
0.1353173833936878	0.6263720884516502	0.5857953641940049
0.3861307040056297	0.8748854266601912	0.5848914496477962
0.7973747405940718	0.9524090845317301	0.4116025369074041
0.5475833166639291	0.7026664832232419	0.4119051440368586
0.5304908552583010	0.5422066844061136	0.4135438741505190
0.7794387858357684	0.7924053586839737	0.4119576239711578
0.5481923316413216	0.8815494500947437	0.4112037749208545
0.7986779989590022	0.6319969465811341	0.4114768356996673
0.6191085839724320	0.9632340113869391	0.5853374266511824
0.8691051751858080	0.7138026243453586	0.5858097140344883
0.8683393179376343	0.5374884373819114	0.5839076867791582
0.6209924762712581	0.7865162043787165	0.5858815028943365
0.6350789754946967	0.6262671565593347	0.5860374589534210
0.8854901562712498	0.8764664505590032	0.5857929858826263
0.4586814631864200	0.2923336234373990	0.5789420669403545

The optimized POSCAR of TM@$CuInP_2S_6$(↓), taking Ni@$CuInP_2S_6$(↓).

2\2\1\CIPS

1.00000000000000

12.1752004622999994 0.0000000000000000 0.0000000000000000

0.0000000000000000 21.1177997588999986 0.0000000000000000

0.0000000000000000 0.0000000000000000 19.4197006226000006

Cu In P S Ni

8 8 16 48 1

Direct

0.4524480804800943 0.2893281438833452 0.4349657826894238

0.2071101692197124 0.0412278281333838 0.4376248749124838

0.9768778262228813 0.2944724187293253 0.4317790395399634

0.7091916667627592 0.0432041650154495 0.4364205779879780

0.4590526379812249 0.7921927905446295 0.4374834953625241

0.2126886977821888 0.5425146687327946 0.4373649434651743

0.9590922862468317 0.7924601329005116 0.4374019841023095

0.7105837775519270 0.5437837762354482 0.4380467010801820

0.2111816340544567 0.3768461962068629 0.5119739069800350

0.4518692698888306 0.1245377018181330 0.5127283237582040

0.7140033579065009 0.3761514487087843 0.5170958614919924

0.9543181936696686 0.1258423887273319 0.5091180449431435

0.2082843705474751 0.8757340270026175 0.5116620027072944

0.4606905025948497 0.6261570913288844 0.5103715268340954

0.7083735945090769 0.8761337775879487 0.5121332937808568

0.9601758418447675 0.6266931072997085 0.5122458442670424

0.4620431802281974 0.4584888039739876 0.4437468783001932

0.2076886990565486 0.2080393837864059 0.4421503925210673

0.4607758330221383 0.4597631225932788 0.5596704292715637

0.2047035775214406 0.2094265177978594 0.5577582251630691

0.9610191715086868 0.4611738941321531 0.4460328863597413
0.7065675379170250 0.2086208129734477 0.4411791379645730
0.9626216380648048 0.4605823970608463 0.5619549941003841
0.7033024290929820 0.2083154426534925 0.5565313670475488
0.4585878873688837 0.9588780930633101 0.4455141874871420
0.2099475301493666 0.7093432004668150 0.4442143952368943
0.4576295747976257 0.9584367130273254 0.5611402983443236
0.2105539092942454 0.7092791820722261 0.5598432827262452
0.9579822035951087 0.9588505921843347 0.4443025688837963
0.7100556317146975 0.7097307099458632 0.4443227211716670
0.9580902710190947 0.9592534818099840 0.5598862101874873
0.7096575403081548 0.7094725807241773 0.5599342135877065
0.3012824085597380 0.4525500254808271 0.4122658237019742
0.0486735555399409 0.2011230706832718 0.4082789843079787
0.0288296631124312 0.0420357254883972 0.4119688030998122
0.2759821424432288 0.2924152780278717 0.4107416557926239
0.0558401115342030 0.3865449847437981 0.4117766471712405
0.2969919772746403 0.1300510494897001 0.4124354407023881
0.1235237147030628 0.4651770511839984 0.5877188729296630
0.3648304231154166 0.2146950042755675 0.5855594608689249
0.3683763337217212 0.0356722205109083 0.5882687592381239
0.1165461331334738 0.2874515208223065 0.5828276487046099
0.1312849343553635 0.1271631486878765 0.5848267533170536
0.3868273547515685 0.3775594891899589 0.5875032253834798
0.8007930088423754 0.4545848999349551 0.4149249621762104
0.5364739853759082 0.1957432049405123 0.4044243760474365
0.5293631661660294 0.0423096640717022 0.4138800311939599
0.7970500380974265 0.2977949549718135 0.4222985959561576
0.5552217274597651 0.3771313299824361 0.4186016675978502
0.7993135985602078 0.1322545634788532 0.4095360118905947

0.6205057247096126	0.4650293289957463	0.5885155653067704
0.8633247243024583	0.2124909140207729	0.5850775407205395
0.8704170317420176	0.0370127149036289	0.5862994925689740
0.6161947937506346	0.2854683128780837	0.5849705165586668
0.6318779017251132	0.1250737884104748	0.5830544140201561
0.8905154276322789	0.3784304021720325	0.5912036632168618
0.2979506729686857	0.9524097603254196	0.4132401698532666
0.0489946761901308	0.7032476850629200	0.4128242909543179
0.0330444977926837	0.5444898562334928	0.4147418346437766
0.2803924713819336	0.7928751395651310	0.4125296302428057
0.0484116576406298	0.8818191860879416	0.4127560725900186
0.3004212297736370	0.6323526400010748	0.4120352821557043
0.1186674854720609	0.9640917313483142	0.5865698273743384
0.3712418796959771	0.7140681311639180	0.5861642483754366
0.3729789497281072	0.5377051318790129	0.5855290750672533
0.1222806120385706	0.7868051525519768	0.5867346322534260
0.1375505701680930	0.6269228791990399	0.5870005688187961
0.3847719531716225	0.8757491096088638	0.5873476090034114
0.7969558625904015	0.9529130523573990	0.4130143749396507
0.5493082359346255	0.7031422701463307	0.4122631808198769
0.5324837802143499	0.5419997418860217	0.4118246891585531
0.7803181722241311	0.7933744653227353	0.4128986349685848
0.5485651102462987	0.8817481290339104	0.4137345471915038
0.8004064643996155	0.6327843357113015	0.4128114508693635
0.6179140489378474	0.9634159958325641	0.5883281270928316
0.8701192979990280	0.7146302426306133	0.5869705994410711
0.8746333728790194	0.5381930248610547	0.5886558397806044
0.6216570055694501	0.7869516004801549	0.5869965545554823
0.6372039424193071	0.6265791487490576	0.5861340393230571
0.8855078343011050	0.8765819798674064	0.5868868610890190

0.6349718207318499 0.2789823386282279 0.3821868287096172

INCAR for structural optimization.

SYSTEM = CIPS

ISTART=0

ICHARG=2

LWAVE= .False.

LCHARG=.False.

NPAR=4

PREC = Accurate

ISMEAR = 0

SIGMA = 0.1

ENCUT = 400

NSW = 100

EDIFFG = -0.01

EDIFF = 1.E-5

ISIF = 3

IBRION = 2

IVDW=1

INCAR for static state calculation.

SYSTEM = TM@CIPS

ISTART=0

ICHARG=2

LWAVE= .TRUE.

LCHARG=.TRUE.

NPAR=4

PREC = Accurate

SYMPREC = 1E-4

ISMEAR = 0

SIGMA = 0.01

ENCUT = 400

ISPIN = 2

NEDOS=2000

LORBIT=11

LVHAR=.TRUE.

LAECHG= .TRUE.

EDIFF = 1.E-5

Reference

[1] C.F. Fu, J.Y. Sun, Q.Q. Luo, X.X. Li, W. Hu, J.L. Yang, Nano Letters, 2018, 18(10), 6312-6317.

[2] N. A. Spaldin, J. Solid State Chem, 2012, 195, 2-10.

[3] R. Resta, Rev. Mod. Phys, 1994, 66, 899.

[4] R.D.K. Smith, D. Vanderbilt, Physical Review B, 1993,47(3), 1651-1654.